Modeling of He distribution in the edge plasma of MAST

V. Rozhansky[1], P. Molchanov[1], S. Voskoboynikov[1], A. Kirk[2], H. Meyer[2], D. Coster[3]

[1]*St.Petersburg State Polytechnical University, Polytechnicheskaya 29, St.Petersburg, Russia*
[2]*EURATOM/CCFE Fusion Association, Culham Science Centre, Abingdon, Oxon, OX14 3DB, UK*
[3]*Max-Planck Institut für Plasmaphysik, EURATOM Association, D-85748 Garching, Germany*

Introduction

Impurities are used in the Doppler spectroscopy method to measure toroidal and poloidal rotation velocities and radial electric field in the vicinity of the separatrix [1]-[4]. On MAST such measurements were performed by means of a helium puff [1]. To understand the distribution and transport of impurities near the separatrix and in the scrape-off layer (SOL) simulations were performed with the B2SOLPS5.2 transport code. A MAST H-mode shot has been chosen where the active Doppler spectroscopy experiments were made. As was shown previously [5] the distribution of impurities strongly differs from the standard neoclassical one in the plasma with steep density gradients even in the absence of turbulent transport and sources. In particular, a significant asymmetry in LFS-HFS impurity distribution and decoupling in parallel velocities of the impurities and the main ions was predicted. Similar predictions were made in [6]. The simulations with B2SOLPS5.2 reported below demonstrate that for the spherical tokamak these effects are strongly amplified and LFS-HFS asymmetry in impurity distribution becomes very strong. A big difference in toroidal rotation of the impurities and that of the main ions is also observed. The obtained results are interpreted on the basis of the analysis of the parallel momentum and continuity equations for impurities. The simulations are consistent with the counter-current toroidal rotation of He ions measured in the experiments. The radial electric field obtained in the simulations is compared with the measured radial electric field. The shapes are similar; however the simulated electric field is larger in absolute value.

Simulation results

A typical H-mode shot 18751 has been chosen for simulation. The electron density and temperatures, and toroidal rotation velocity were specified at the core side of the simulation domain in accordance with the experimental observations. The transport coefficients with the drop in the barrier region were chosen to match the density and temperature profiles as well

as the power coming from the core, Fig.1. The density and electron temperature profiles are shown in Figs. 2-3. A The He^{+2} ion density of $4 \cdot 10^{16} m^{-3}$ has been put as a boundary condition at the core side of the simulation domain to specify the He puff. The He^{+2} density profiles, Figs. 4-5, reveal a strong LFS-HFS asymmetry. The He^{+2} parallel velocity differs from that of the main ions both in absolute value and in poloidal dependence, Fig. 6. The He^{+1} parallel velocity also differs from those of the main ions, Fig. 7. The measured radial electric field profile [1] and simulated one are shown in Fig. 8.

Discussion

The degree of coupling of the impurities to the main ions is determined by the parallel momentum and by the particle balance equations. At the core side, according to the standard neoclassical theory, [7]-[8] the poloidal $\vec{E} \times \vec{B}$ and diamagnetic drifts of impurities are closed by their parallel Pfirsch-Schlueter (PS) flows, so the parallel velocities of all impurities should be different and should differ from the parallel velocity of the main ions. The radial neoclassical flux is caused by the toroidal component of the friction force and thermal force. On the other hand, standard neoclassical theory is not applicable to the steep gradient case [5] when (ρ_{ci} is the ion gyroradius, L is the spatial scale, Z is the charge number)

$$\rho_{ci} B_T / (Z^2 B_p L) > 1. \tag{1}$$

This is the case for the edge barrier region. In H-mode the parallel pressure gradient for impurities that is necessary to drive the impurity PS flow requires such a strong poloidal variation of impurity ions that is inconsistent with the particle balance equation. As a result according to [5] the parallel impurity flow should differ from the PS one. The poloidal $\vec{E} \times \vec{B}$ and diamagnetic drifts of impurities are not closed by the parallel PS flows and are compensated by the HFS rise of impurity density with respect to LFS, since the poloidal velocity is smaller at the HFS.

Since the ratio of HFS-LFS magnetic fields is of the order of 4, in a spherical tokamak the HFS-LFS asymmetry should be very strong. It would be expected that asymmetry of He ions density would also be of the same order to keep the poloidal flow constant. That is approximately what is observed in the simulations in Figs. 4-5 for He^{+2}. In spite of the fact that the core boundary condition prescribes the poloidally independent value $4 \cdot 10^{16} m^{-3}$, closer to the separatrix the asymmetry dramatically increases. Radial transport and ionization sources make the situation more complicated. To check the relative role of various

contributions the drift terms were switched off. In this test case the poloidal asymmetry has been strongly reduced, which demonstrates the key role of the drift effects. The poloidal asymmetry in He^{+1} is also strong. The strong poloidal pressure gradient causes parallel flows of He ions from the HFS to the LFS that are maximal at the upper and lower parts of the flux surfaces. The pressure gradient is balanced by inertia. In addition the thermal force from the main ions is directed from the top to the bottom due to the hotter ion temperature at the bottom caused by neoclassical effects [9]. The thermal force causes impurity flows in the counter current direction and is balanced by the friction with the main ions, Fig. 9. As a result the parallel He flows have a complicated poloidal distribution which is different from the PS flows. At the LFS the parallel velocities of He ions should be shifted in the counter-current direction. This is observed in the simulations, Fig.7. The He^{+1} parallel velocity becomes positive (counter current) in accordance with the observation [1]. Parallel flows different from the PS ones were observed on Cmod [4], and the HFS-LFS asymmetry of the order 2-3 has been estimated.

The structure of the radial electric field is similar to the measured one but the absolute value of the dip in the experiments is smaller than the calculated one.

Conclusions

The strong LFS-HFS asymmetry of the He ions distribution in the edge transport barrier region is obtained in the simulations. The parallel velocities of impurities are quite different from their PS velocities. At the LFS the parallel velocities of impurities are shifted in the counter current direction with respect to those of the main ions.

References

[1] H. Meyer Journal of Physics: Conference Series **123** (2008) 012005

[2] T. Putterich, E. Wolfrum, R Dux, C.F. Maggi and ASDEX Upgrade Team Phys. Rev. Lett. **102** (2009) 025001

[3] R.M. Mcdermott et al Phys. Plasmas **16** (2009) 056103

[4] K. D. Marr et al Plasma Phys. Contr. Fus. **52** (2010) 055010

[5] V. Rozhansky Sov. Journ. Plasma Phys. **5** (1979) 771 ; **6** (1980) ; **10** (1984) 254

[6] T Fulop, P. Helander Phys. Plasmas **8** (2001) 3305

[7] P. H. Rutherford Phys. Fluids **17** (1974) 1781

[8] S. P. Hirschman, D.J. Sigmar Nuclear Fus. **5** (1981) 771

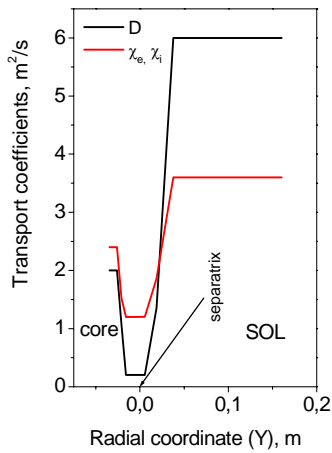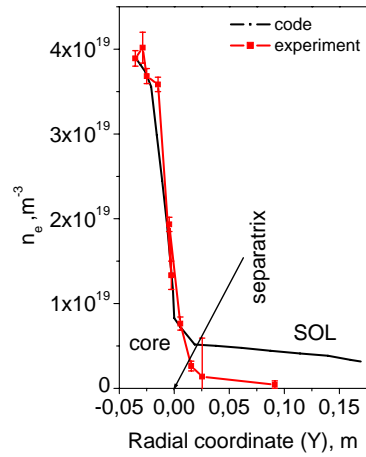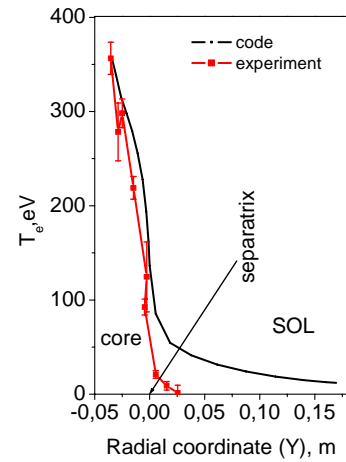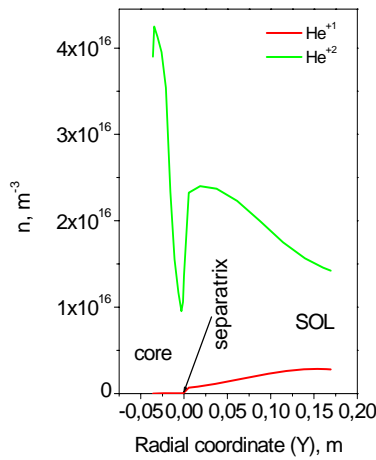[9] V. Rozhansky et al Proc. 31st Conf. on Plasma Phys. ECA **28G** (2004) P.-4.198
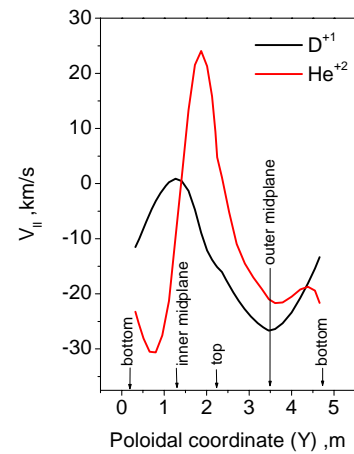
Fig.1

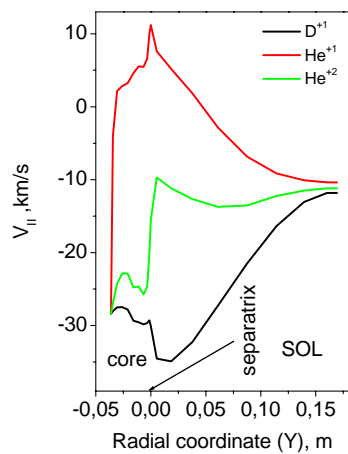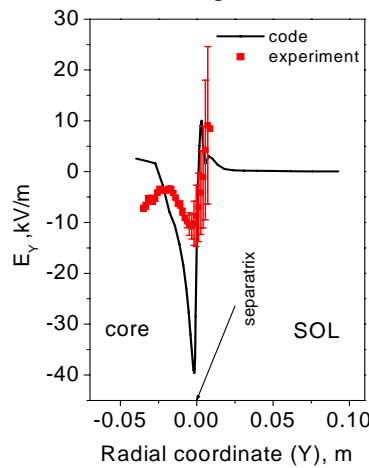Fig.2

Fig.3

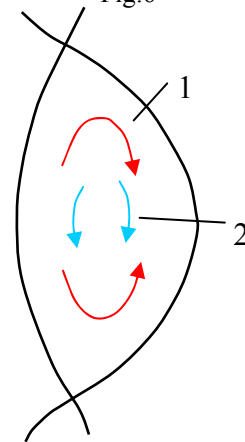Fig.4
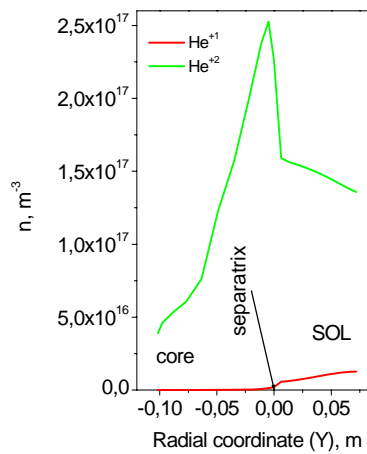
Fig.5

Fig.6

Fig.7

Fig.8

Fig.9

Fig.1. Transport coefficients at the outer midplane. Fig.2. Electron density profile at the outer midplane. Fig.3. Electron temperature profile at the outer midplane. Fig.4. He ions density profile at the outer midplane. Fig.5. He ions density profile at the inner midplane. Fig.6. The poloidal dependence of He^{+2} parallel velocity in the core (2cm inside from the separatrix at the outer midplane). Fig.7. Parallel ion velocities profile at the outer midplane in the core. Fig.8. Comparison of the code and experimental electric field at the outer midplane; Fig.9. Poloidal projection of the parallel He^{+2} flows. 1 – pressure-driven flows; 2 – caused by the thermal force.